Supplementary Table 1.

Data collection, phasing and refinement statistics for *A. locustae* Spt6 tandem SH2

	Native	$KAu(CN)_2$	$(CH_3)_3PbAc$
Data collection			
Space group	$P2_12_12$	$P2_12_12$	$P2_12_12$
Cell dimensions			
a, *b*, *c* (Å)	59.10,49.78,59.53	59.84,50.56,59.51	59.29,50.20,59.48
α, β, γ (°)	90, 90, 90	90, 90, 90	90, 90, 90
Resolution (Å)	32-2.20 (2.28-2.20)[a]	32-2.45 (2.54-2.45)[b]	32-2.45 (2.54-2.45)[b]
R_{sym} or R_{merge}	4.2 (26.0)	3.5 (15.7)	4.3 (18.7)
$I / \sigma I$	52.9 (7.3)	33.2 (9.8)	46.7 (11.5)
Completeness (%)	98.9 (99.9)	95.7 (95.0)	99.7 (99.9)
Redundancy	6.6 (6.7)	3.7 (3.4)	5.6 (5.2)
Refinement			
Resolution (Å)	32-2.20		
No. reflections	8803		
R_{work} / R_{free}	0.225 / 0.266		
No. atoms			
Protein	1457		
Ligand/ion	11		
Water	20		
B-factors			
Protein	29.35		
Ligand/ion	48.10		
Water	31.63		
R.m.s deviations			
Bond lengths (Å)	0.016		
Bond angles (°)	1.627		

[a] Values in parentheses are for the highest-resolution shell.

Supplementary Table 2.

S. cerevisiae strains.

Strain	**Genotype**
FY2808	*MAT***a***/MATα his3Δ200/" leu2Δ1/" lys2-128δ/" trp1Δ163/" ura3-52/" KanMx-GAL1pr-FLO8-HIS3/"*
FY2809	*MATα his3Δ200 leu2Δ1 lys2-128δ trp1Δ163 ura3-52 KanMx-GAL1pr-FLO8-HIS3*
FY2810	*MATα his3Δ200 leu2Δ1 lys2-128δ trp1Δ163 ura3-52 KanMx-GAL1pr-FLO8-HIS3 SPT6::TAP-NatMx*
FY2811	*MATα his3Δ200 leu2Δ1 lys2-128δ trp1Δ163 ura3-52 KanMx-GAL1pr-FLO8-HIS3 spt6ΔTandem::TAP-NatMx* (Last 201 codons of *SPT6* deleted and replaced with TAP tag)
FY2812	*MATα his3Δ200 leu2Δ1 lys2-128δ trp1Δ163 ura3-52 KanMx-GAL1pr-FLO8-HIS3 spt6ΔSH2$_2$::TAP-NatMx* (Last 101 codons of *SPT6* deleted and replaced with TAP tag)
FY653	*MATα his4-912δ lys2-128δ ura3-52 leu2Δ1*
FY2796	*MAT***a***/MATα his3Δ200/" leu2Δ1/" lys2-128δ/" trp1Δ163/" ura3-52/" KanMx-GAL1pr-FLO8-HIS3/" SPT6::TAP-NatMx/SPT6* (Note: Diploid strain with one copy of wild-type *SPT6* and one copy of TAP-tagged *SPT6* allele.)
FY2797	*MAT***a***/MATα his3Δ200/" leu2Δ1/" lys2-128δ/" trp1Δ163/" ura3-52/" KanMx-GAL1pr-FLO8-HIS3/" spt6 ΔTandem::TAP-NatMx/SPT6* (Note: last 201 codons of *SPT6* deleted and replaced with TAP tag. Diploid strain with one copy of wild-type *SPT6* and one copy of truncated *spt6* allele.)
FY2798	*MAT***a***/MATα his3Δ200/" leu2Δ1/" lys2-128δ/" trp1Δ163/" ura3-52/" KanMx-GAL1pr-FLO8-HIS3/" spt6ΔSH2$_2$::TAP-NatMx/SPT6* (Note: last 101 codons of *SPT6* deleted and replaced with TAP tag. Diploid strain with one copy of wild-type *SPT6* and one copy of truncated *spt6* allele.)

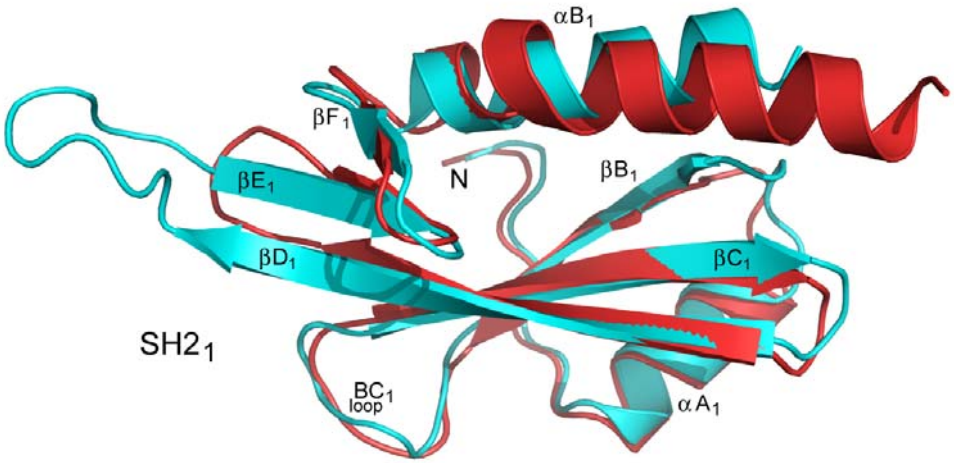

Supplementary Figure 1. Superposition of the $SH2_1$ domains from *A. locustae* and *C. glabrata*. The $SH2_1$ domains from *Antonospora locustae* (red) and *Candida glabrata* (cyan) have been superposed and are represented as ribbons. Secondary structure elements are labeled according to the nomenclature of SH2 domains. Major structural differences include: (i) extended βD_1 and βE_1 strands in the case of the *C. glabrata* $SH2_1$ and (ii) a kink in the αB_1 helix of the *A. locustae* $SH2_1$ which is most likely imposed by the interaction between the $SH2_1$ and $SH2_2$ domains and which induces a different path for the two αB_1 helices.

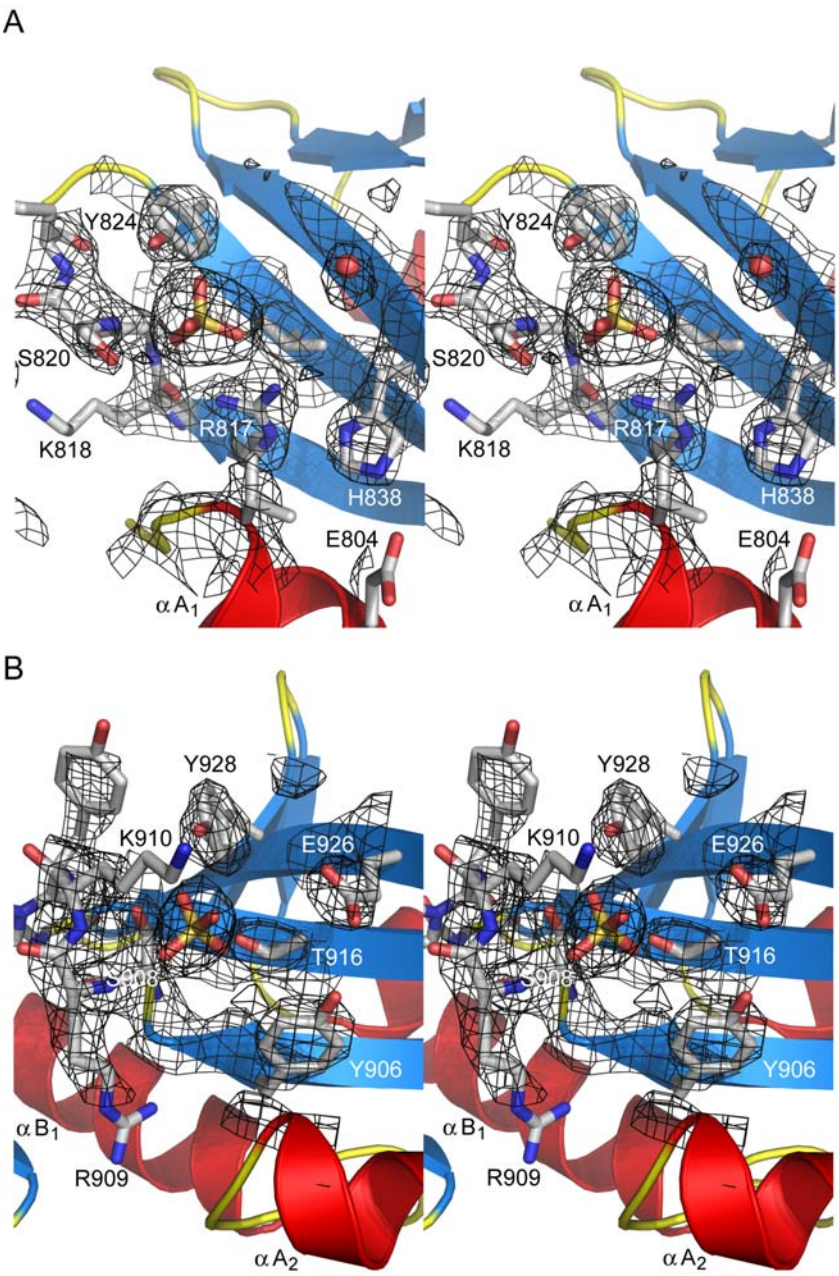

Supplementary Figure 2. Stereo views of the phosphate binding pockets of (A) the $SH2_1$ and (B) the $SH2_2$ domains. The domains are represented as ribbons with the exception of the central part of the BC loops which are represented as sticks. The bound sulfate ions and the residues coordinating these ions are shown as sticks and labeled. Water molecules are shown as spheres. The 2Fo-Fc electron density surrounding the sulfate ions is shown, contoured at 1 σ.

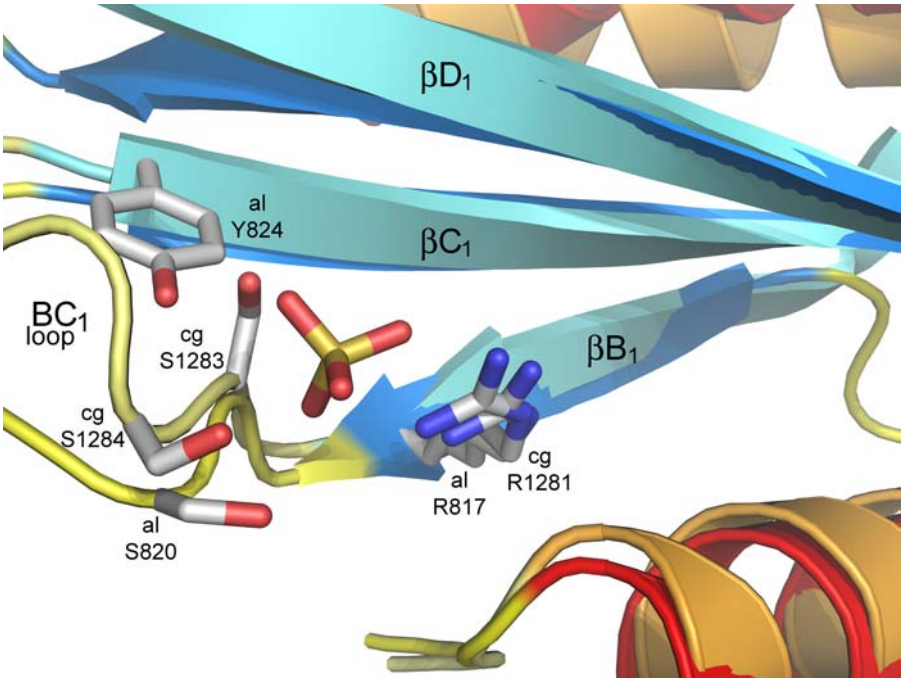

Supplementary Figure 3. Superposition of the phosphate binding pockets of the $SH2_1$ domains from *A. locustae* and *C. glabrata*. The two phosphate binding pockets of the $SH2_1$ domains from *Antonospora locustae* (al) and *Candida glabrata* (cg) have been superposed and the residues putatively involved in phosphate binding are shown as sticks and labeled. The bound sulfate ion observed in the *A. locustae* structure of the Spt6 tandem SH2 is shown. Strict correspondence is observed for arginines alR817 and cgR1281 and serines alS820 and cgS1284. This is not the case for the *A. locustae* tyrosine alY824 which coordinates a sulfate ion in the tandem SH2 structure and which is not conserved throughout evolution. However, the serine cgS1283 in the *C. glabrata* BC_1 loop, which is conserved throughout evolution except in *A. locustae*, is perfectly positioned to replace alY824 for coordinating a phosphate ion. This positioning is notably due to a different conformation of the BC_1 loop which is one residue longer in *C. glabrata* - and in most Spt6 proteins - than in *A. locustae*.

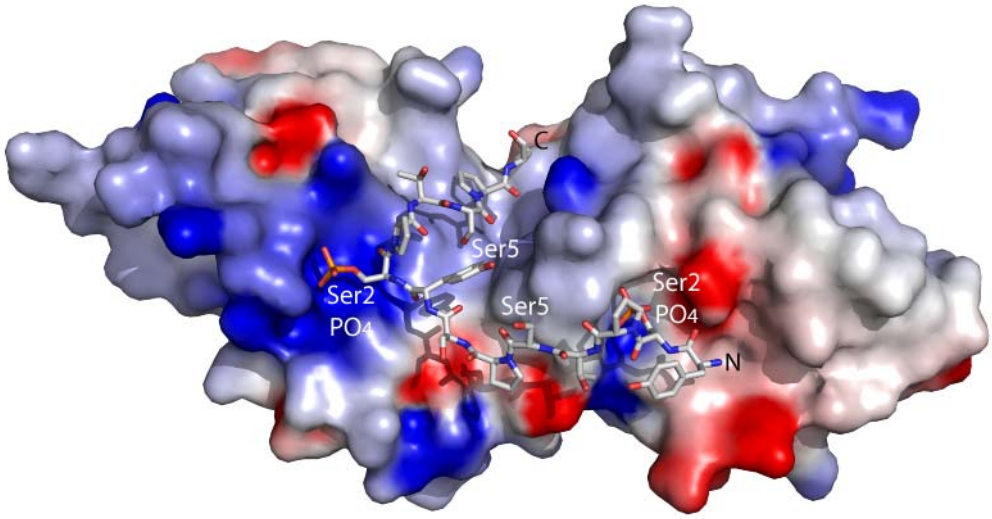

Supplementary Figure 4. Tentative modeling of the interaction of the tandem SH2 with two consecutive Ser2-phosphorylated CTD repeats. In this model, the phosphorylated Ser2 of the first repeat binds to the phosphoresidue binding pocket of the $SH2_2$ domain. The repeat goes in an extended conformation towards the phosphoresidue binding pocket of the $SH2_1$ domain where the phosphorylated Ser2 of the second repeat binds. The rest of the second repeat is recognized by the grove between both SH2 domains where specific binding might occur.

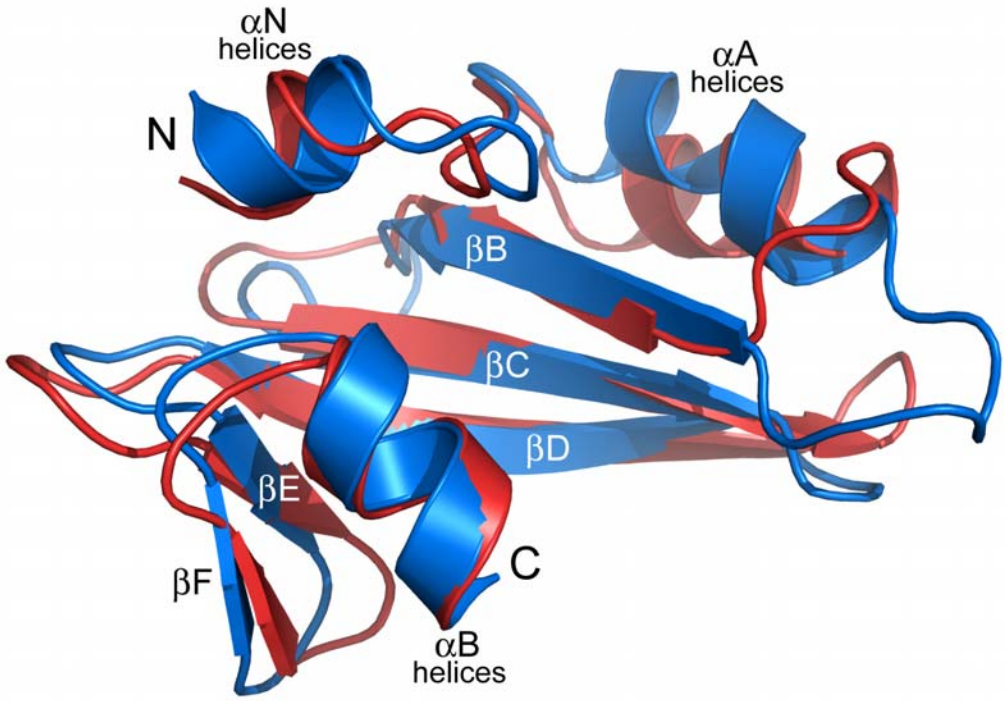

Supplementary Figure 5. Superposition of the $SH2_1$ and $SH2_2$ domains of *A. locustae* Spt6 tandem SH2. The $SH2_1$ (red) and $SH2_2$ (blue) domains of the tandem SH2 from *Antonospora locustae* Spt6 have been superposed and are shown as ribbons. For the superposition, the long αB_1 helix connecting both domains has been divided in three parts: the N-terminal part forms the normal αB_1 helix of the $SH2_1$, the central part has been removed, and the C-terminal part has been considered as a small αN helix of the $SH2_2$. Upon superposition, the αB helices but also the αN helices superpose nicely, suggesting that the tandem SH2 has been created through duplication of an ancestral SH2 domain followed by the evolution of the $SH2_2$ domain into a non canonical SH2 motif.